Scientific Research Publishing

Modeling and Numerical Simulation of Material Science, 2024, 14, 39-57
https://www.scirp.org/journal/mnsms
ISSN Online: 2164-5353
ISSN Print: 2164-5345

Molecular Dynamics, Diffusion Coefficients and Activation Energy of the Electrolyte (Anode) in Lithium (Li and Li^+), Sodium (Na and Na^+) and Potassium (K and K^+)

Alain Second Dzabana Honguelet[1,2,3*], Timothée Nsongo[1,2,4], Bitho Rodongo[1,2,4], Earvin Loumbandzila[1,2]

[1]Faculty of Science and Technology, Marien Ngouabi University, Brazzaville, Congo
[2]Research Group on The Physical and Chemical Properties of Materials, Brazzaville, Congo
[3]Association Alpha Sciences Beta Technologies, Brazzaville, Congo
[4]Centre for Geological and Mining Research, Brazzaville, Congo
Email: *second_alain@yahoo.fr

How to cite this paper: Honguelet, A.S.D., Nsongo, T., Rodongo, B. and Loumbandzila, E. (2024) Molecular Dynamics, Diffusion Coefficients and Activation Energy of the Electrolyte (Anode) in Lithium (Li and Li^+), Sodium (Na and Na^+) and Potassium (K and K^+). *Modeling and Numerical Simulation of Material Science*, **14**, 39-57.
https://doi.org/10.4236/mnsms.2024.141002

Received: July 14, 2023
Accepted: November 27, 2023
Published: November 30, 2023

Abstract

This work is a simulation modelling with the LAMMPS calculation code of an electrode based on alkali metals (lithium, sodium and potassium) using the MEAM potential. For different multiplicities, two models were studied; with and without gap. In this work, we present the structural, physical and chemical properties of the lithium, sodium and potassium electrodes. For the structural properties, the cohesive energy and the mesh parameters were calculated, revealing that, whatever the chemical element selected, the compact hexagonal hcp structure is the most stable, followed by the face-centred cubic CFC structure, and finally the BCC structure. The most stable structure is lithium, with a cohesion energy of −6570 eV, and the lowest bcc-hcp transition energy of −0.553 eV/atom, followed by sodium. For physical properties, kinetic and potential energies were calculated for each of the sectioned chemical elements, with lithium achieving the highest value. Finally, for the chemical properties, we studied the diffusion coefficient and the activation energy. Only potassium followed an opposite order to the other two, with the quantities with lacunae being greater than those without lacunae, whatever the multiplicity. The order of magnitude of the diffusion coefficients is given by the relationship $D_{Li} > D_{Na} > D_k$ for the multiplicity 6*6*6, while for the activation energy the order is reversed.

Keywords

Molecular Dynamics, Diffusion Coefficients, Activation Energy, Lithium,

Alkali Metals, MEAM Potential

1. Introduction

Lithium batteries are widely used in electronic devices such as mobile phones and electric vehicles, and studies are continuing to increase their efficiency and stability [1]; computational models can be used to analyse lithium battery materials. Recent studies have established the link between thermal conductivity and diffusion coefficients and the energy of electrolyte activation [2] [3].

In today's batteries, the use of lithium at the negative electrode, combined with a carefully chosen cathode (high potential), makes it possible to obtain the highest values of mass energy and a much higher voltage of around 4 V than that of alkaline batteries of around 1.5 V [4].

However, the use of lithium as a negative electrode requires specificsafety devices and instructions to be followed during transport, use and recycling [5] [6]. The use of a battery includes the installation of a depressurisation cap (to prevent explosion following a rise in pressure), electrical devices to prevent excessively high discharge rates (this involves an element called a PTC which is connected in series and whose electrical resistance increases with temperature), or accidental recharging (diode), or a rise in temperature (stopping the discharge by a breaker). Among the many existing systems, we can distinguish three families of lithium batteries, depending on the nature of the cathode and/or the electrolyte used: liquid cathode batteries, solid cathode batteries and solid electrolyte batteries; to answer this problem relating to lithium, we thought we would study the alkaline metals close to lithium.

Batteries are not new to the Research Group on the Physical and Chemical Properties of Materials. The group's predecessors have already carried out a practical study using basic solutions to obtain electrical energy. They have also been studied in previous years at the Faculty of Science and Technology in Congo Brazzaville.

In our study, based on the simulation of an electrochemical cell, we compare the properties of the lithium anode with those of the neighbouring alkali metals: Potassium and Sodium. We also compare the activation energies of systems without gaps with those of systems with a gap in the centre of the lattice for any multiplicity.

2. Method

2.1. Molecular Dynamics [7]

Molecular Dynamics is a formidable tool for investigating matter at the atomic scale. It involves numerically simulating the evolution of a system of particles as a function of time, with the aim of predicting and understanding experimental results. It makes it possible to highlight structural arrangements or dynamic

phenomena that are still inaccessible to current experimental observation methods (EXAFS, NMR, Atom Probe Tomography—APT), especially for amorphous materials such as glasses. This move into the digital world requires time to be discretised in order to solve Newton's equations governing the motion of each particle. The principle of Molecular Dynamics is then to integrate these discretised equations, under various physical constraints, using various algorithms which can be found in various reference books such as that by Griebel *et al.* 12, a clear work containing examples and practical applications, useful for anyone wanting to start writing their own Molecular Dynamics programme. The methods presented are those used in this thesis. After an explanation of the "Velocity-Störmer-Verlet" algorithm, which strikes a balance between robustness, practicality and performance, a presentation of the Nosé-Hoover thermostat and barostat shows how the temperature and pressure of a material can be controlled in a fully integrated way. A key point in the simulations is the appropriate parameterisation of interatomic interactions. The interaction potential used must above all take account of known properties in order to be able to predict those that are not, or to be able to explain a phenomenon that is still poorly understood. Calculating these interactions during simulation, particularly electrostatic interactions, is the step that requires the most numerical computing resources. The method developed by Wolf overcomes this limitation and opens up the field of simulations on much larger size and time scales. These methods and algorithms are finally being applied to the modelling of silica materials, in particular glasses, where certain properties and experimental behaviours are reproduced with acuity.

a) Algorithms for integrating Newton's equations [8]

In Classical Molecular Dynamics, each particle is considered as a point mass interacting at a distance with others via an effective interaction potential. In an ensemble of N interacting particles, the motion of particle i of mass m_i (with i = 1 to N) is governed by the equation :

$$m_i \frac{\mathrm{d}^2 x_i}{\mathrm{d}t^2} = F_i \tag{1}$$

with the convention $x_i = \vec{x_i}$ for the position vector, and F_i is the vector resulting from all the forces applied to particle i.

b) Standard Störmer-Verlet method [9] [10]

The basic numerical method for solving the equations of motion is to perform a 3rd order Taylor series expansion of the position x around the date t, i.e. at $t \pm \delta t$ (with δt small):

$$\begin{cases} x(t+\delta t) = x(t) + \delta t \dfrac{\mathrm{d}x}{\mathrm{d}t} + \dfrac{1}{2}\delta t^2 \dfrac{\mathrm{d}^2 x}{\mathrm{d}t^2} + \dfrac{1}{6}\delta t^3 \dfrac{\mathrm{d}^3 x}{\mathrm{d}t^3} \\ x(t-\delta t) = x(t) - \delta t \dfrac{\mathrm{d}x}{\mathrm{d}t} + \dfrac{1}{2}\delta t^2 \dfrac{\mathrm{d}^2 x}{\mathrm{d}t^2} - \dfrac{1}{6}\delta t^3 \dfrac{\mathrm{d}^3 x}{\mathrm{d}t^3} \end{cases} \tag{2}$$

By adding up and grouping the terms, we obtain:

$$\frac{\mathrm{d}^2x}{\mathrm{d}t^2}=\frac{1}{\delta t^2}\left[x\left(t+\delta t\right)-2x\left(t\right)+x\left(t-\delta t\right)\right] \tag{3}$$

Time is discretised using a time step δt (of the order of femto seconds in Molecular Dynamics). At iteration n, the date is expressed by $t_n=n\delta t$, the position vector by x_i^n, the velocity vector by v_i^n and the force vector by F_i^n. After this discretisation and digitisation, the previous equation becomes, for the date $t_{n+1}=t_n+\delta t$:

$$m_i\frac{1}{\delta t^2}\left(x_i^{n+1}-2x_i^n+x_i^{n-1}\right)=F_i^n \tag{4}$$

In the same way, but subtracting the terms this time, we obtain the expression for speed:

$$\frac{\mathrm{d}^2x}{\mathrm{d}t^2}=\frac{x\left(t+\delta t\right)-x\left(t-\delta t\right)}{2\delta t}=v_i^n=\frac{x_i^{n+1}-x_i^{n-1}}{2\delta t} \tag{5}$$

This is the standard form of the Störmer-Verlet method for integrating Newton's equations:

$$\begin{cases}x_i^{n+1}=2x_i^n-x_i^{n-1}+\dfrac{\delta t^2}{m_i}F_i^n\\ v_i^n=\dfrac{x_i^{n+1}-x_i^{n-1}}{2\delta t}\end{cases} \tag{6}$$

2.2. Modified Embedded Atom Method and Interatomic Potential [11] [12]

Interatomic potentials are of vital importance for simulations that model the properties of materials. The basis of these potentials is density function theory (DFT), which postulates that energy is a function of electron density. By knowing the electron density of an entire system, we can determine the potential energy of a system:

$$U=\left[\rho\left(r\right)\right] \tag{7}$$

$$E\left[\rho\left(r\right)\right]=Ts\left[\rho\left(r\right)\right]+J\left[\rho\left(r\right)\right]+Exc\left[\rho\left(r\right)\right]+Eext\left[\rho\left(r\right)\right]+E_{ii}\left[\rho\left(r\right)\right] \tag{8}$$

where E is the total energy, Ts is the kinetic energy of the single particle, J is the Hartree electron-electron energy, Exc is the exchange correlation function, $Eext$ is the electron-ion coulombic interaction, and E_{ii} is the ion-ion energy.

On this basis, the Embedded Atom Method (EAM) was created by assuming that an atom can be embedded in a homogeneous electron gas and that the change in potential energy is a function of the electron density of the embedded atom which can be approximated by an embedding function. In a crystal, however, the electron density is not homogeneous, so the EAM potential replaces the background electron density with the electron densities of each atom and supplements the embedding energy with a repulsive pair potential to represent the core-core interactions of the atoms.

With a simple linear superposition of the electron densities of the atoms as the background electron density, the EAM is governed by the following equations:

$$R_{ii} = \left| r_i - r_j \right| \tag{9}$$

$$\overline{\rho}_i = \sum \left(R_{ij} \right)_j \tag{10}$$

$$U = \sum \left(\overline{\rho}_i \right)_i + \frac{1}{2} \sum \phi \left(R_{ij} \right)_{i,j} \tag{11}$$

where R_{ij} is the distance between atoms *i* and *j*, $r_{i,j}$ is the position between atoms *i* and *j*, $\overline{\rho}_i$ is the fundamental electron density, and ϕ is the pair interaction potential.

However, EAM does not do an excellent job of simulating materials with significant directional binding, which includes most metals. In order to correctly simulate metals, the modified embedded atom method was created, which allows the background electron density to depend on the local environment instead of assuming a linear superposition.

In the MEAM formalism, we consider a set of atoms forming a cluster. Each atom is immersed in the electron density created by the other atoms. The total energy depends on two factors: the immersion potential and the pair interaction potential:

$$E = \sum\nolimits_i F_i \left(\overline{\rho}_i \right) + \frac{1}{2} \sum\nolimits_{j \neq 1} \phi_{ij} \left(R_{ij} \right) \tag{12}$$

For an atom *i*, F_i is the immersion potential, $\overline{\rho}_i$ is the fundamental electron density. $\phi_{ij} \left(R_{ij} \right)$ is the pair interaction potential between two atoms *i* and *j*, at distance R_{ij}.

The immersion potential is calculated as follows:

$$F_i \left(\overline{\rho}_i \right) = AE_c \frac{\overline{\rho}_i}{\rho_0} Ln \left(\frac{\overline{\rho}_i}{\rho_0} \right) \tag{13}$$

where:

A is a parameter that can be adjusted according to the experimental data;

E_c is the sublimation energy;

ρ_0 the electron density in the reference structure;

$\overline{\rho}_i$ the electron density in the real structure.

In MEAM1, interactions in the reference structure are limited to the first neighbourhood. Under these conditions, the atomic positions and bond directions are fixed. The immersion potential depends only on the distance to the first neighbourhood and the number of first neighbours. Consequently, the energy of an atom can be written as a function of *R* as follows:

$$E^u \left(R \right) = F \left[\overline{\rho}_i^0 \left(R \right) \right] + \frac{Z_1}{2} \phi \left(R \right) \tag{14}$$

where Z_1 is the number of first neighbours of the atom.

By calculating $E^u \left(R \right)$ from Rose's equation of state, we can derive the expression for the interaction potential of the pairs as follows:

$$\phi \left(R \right) = \frac{2}{Z_1} \left[E^u \left(R \right) - F \left[\overline{\rho}_i^0 \left(R \right) \right] \right] \tag{15}$$

In MEAM2, we consider second-neighbour interactions in the reference structure and this can be done by adding a screen parameter *S*. From this, the energy of an atom in a reference structure can then be written:

$$E^u(R) = F\left[\bar{\rho}_i^0(R)\right] + \frac{Z_1}{2}\phi(R) + \frac{Z_2 S}{2}\phi(aR) \tag{16}$$

where:

Z_1 is the number of first neighbours in the reference structure;

Z_2 is the number of second neighbours in the reference structure;

a is the ratio of the distances of the second and first neighbours $a = R_2/R_1$;

S is the screen function. For a given reference structure, the screen factor S is constant.

The above equation can be written as:

$$E^u(R) = F\left[\bar{\rho}_i^0(R)\right] + \frac{Z_1}{2}\psi(R) \tag{17}$$

With

$$\psi(R) = \phi(R) + \frac{Z_2 S}{Z_1}\phi(aR) \tag{18}$$

From the value $\psi(R)$ the pair interaction potential is calculated iteratively using the following formula:

$$\phi(R) = \psi(R) + \sum_{n=1}(-1)^n \left(\frac{Z_2 S}{Z_1}\right)^n \psi\left(a^n R\right) \tag{19}$$

For a MEAM interatomic potential that describes the relationship for alloys with two or more components, each component needs 13 individual adjustable parameters. In addition, each binary interaction requires at least 14 adjustable parameters. These parameters are used in the calculation of the potential energy described in Equation (2-7) and govern the forces acting on the atoms. These parameters are listed below (see library: parameter).

3. Work Procedure

In this section we present the approach taken to simulate our stack and calculate the activation energies. We paid particular attention to the choice of elements, the various interactions between systems and the composition of the systems.

3.1. Choice of Components

The simulation of the cell begins by determining the nature of the elements to be used as electrodes (anode and cathode) and their melting points. For simplicity's sake, we have chosen alkalis as the anode and their oxides as the cathode; their electronic properties are shown in **Table 1**.

This table shows lithium as the best basic element for electronics. Caesium, which has a similar melting point at room temperature, was quickly eliminated from our calculations.

Table 1. Electronic properties of alkalis.

element	Li	Na	K	Cs
electronegativity	0.98	0.93	0.82	0.79
Melting point	180.54	97.720	63.380	28.440
Vaporisation point	1342	882.9	758.9	671
Electronic affinity	0.618	0.547	0.502	0.472
Ionisation energy	**5 eV**	**5.139**	**4.341**	**3.894**
Thermal conductivity	85 W/mK	140	100	36
Specific heat		1230 J/Kg·K	757	242
Ref. structure		BCC		

3.2. Structure

After choosing the composite elements for the anode and cathode, we selected the structures to be used thanks to the "materials projects" website, which offers a wide range of structures for a single element, as well as a database of the physical and chemical properties of these elements, see Figure 1.

For the anode and cathode, we arbitrarily chose BCC structures in order to be able to compare them without worry. These basic structures were processed using OVITO software to generate "atomic position" data files that could be accessed by our LAMMPS calculation code.

These atomic position data files then underwent secondary processing to generate an order of multiplicity 4 × 4 × 4 and others in which we remove an atom to form the ion of the element treated in the vicinity of the melting point.

3.3. Interactions

The choice of potentials defining the nature of the systems remains essential for any simulation and any physical phenomenon to be interpreted. The Table 2 below shows a set of potentials used in LAMMPS and the nature of the systems used.

Simple elements

The potential file, in Table 3, used in our LAMMPS calculation code is divided into two essential parts: a librairy file and a parameter file, each containing specific types of fixed and adjustable parameters.

File-library

 # DATE: 2012-06-29 DATE: 2007-06-11 CONTRIBUTOR: Greg Wagner, gjwagne@sandia.gov CITATION: Baskes, Phys Rev B, 46, 2727-2742 (1992)

meam data from vax files fcc, bcc, dia 11/4/92

 # elt lat z ielement atwt alpha b0 b1 b2 b3 alat esub asub

 # t0 t1 t2 t3 rozero ibar

Li' 'bcc' 8 3 6.939 2.97244804 1.425 1.00 1.00169907 1.00 3.509 1.65 0.87 1.0 0.26395017 0.44431129 −0.2 1. 0

Na' 'bcc' 8 11 22.9898 3.64280541 2.313 1.00 1.00173951 1.00 4.291 1.13 0.9 1.0 3.55398839 0.68807569 −0.2 1. 0

K' 'bcc' 8 19 39.102 3.90128376 2.687 1.00 1.00186667 1.00 5.344 0.94 0.92 1.0 5.09756981 0.69413264 −0.2 1. 0

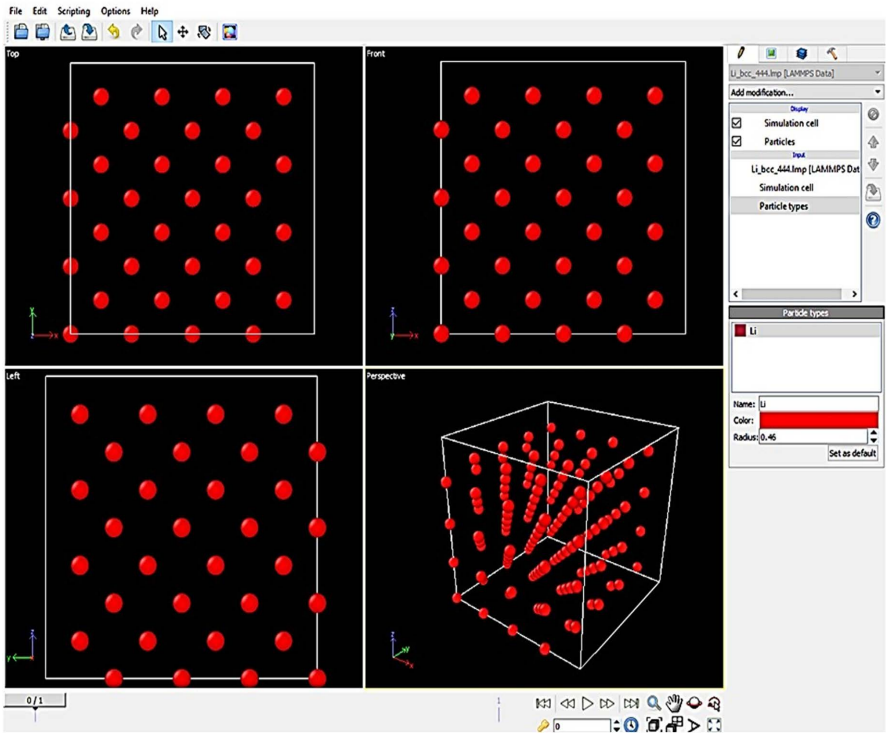

Figure 1. 4*4*4 bcc structure generated by AtomsK under ovito.

Table 2. Potentials and system used.

Potentials	Metals	Semiconductors	Materials Ionic
Embedded Atom			
Modified Embedded Atom			
Stillinger Weber			
Buckingham + coulomb			
Shell Potentials			

Table 3. Additional MEAM parameters.

N°	Parameters	Li	Na	K
1	rc	3.6	43,997	54,797
2	delr	0.1	0.1	0.1
3	augt1	0	0	0
4	erose_form	2	2	2
5	ialloy	2	2	2
6	zbl(1, 1)	0	0	0
7	nn2(1, 1)	1	1	1
8	attrac(1, 1)	0.05	0.05	0.05
9	repuls(1, 1)	0.05	0.05	0.05

Continued

10	Cmin(1, 1, 1)	0.16	0.16	0.16
11	Cmax(1, 1, 1)	2.8	2.8	2.8
12	Ec(1, 1)	1.65	1.13	0.94
13	re(1, 1)	3.02	3821	4874

3.4. Diffusion Coefficients and Activation Energy [13] [14]

The diffusion coefficients were calculated (generated) by gnuplot. Between two consecutive states, the activation energy reflecting the behaviour of the atoms was calculated using the following expression:

$$\begin{cases} \ln D_1 = \ln D_0 - \dfrac{E_a}{k_B T_1} \\ \ln D_2 = \ln D_0 - \dfrac{E_a}{k_B T_2} \end{cases} \tag{20}$$

$$E_a = k_B \frac{T_2 T_1}{T_1 - T_2} \ln \frac{D_1}{D_2} \tag{21}$$

With D_i diffusion coefficient at the time T_i;

E_a activation energy;

k_B boltzman constant.

The activation energy of a chemical reaction is closely linked to its speed. The higher the activation energy, the slower the chemical reaction. This is because the molecules can only complete the reaction once they have reached the top of the activation barrier.

4. Results

In this chapter we present the results as systematically as the working procedure, although several elements were downgraded according to our needs. We therefore thought it reasonable to validate the potentials used for the pure elements, then we set optimum temperatures for the simulation for the anode and cathode; some physical gradations were calculated and represented for the need for more understanding of the diffusion phenomenon for the cell. Finally, the energy and diffusion coefficient were calculated in the vicinity of the operating temperatures of the elements Lithium, Potassium and Sodium.

4.1. Structural Properties

a) Validation of potential parameters

Here we have calculated the cohesion energies for BCC structures of the elements to be used as alloys at the anode. **Table 4** shows the cohesive energy of the structures selected in the BCC, FCC and HCP crystallographic structures. This was also done for 4*4*4 and 6*6*6 multiplicities for a triclinic BCC phase.

Table 4. Cohesion and transition energies[15] [16].

							triclinic	
				1*1*1			4*4*4	6*6*6
	bcc	fcc	hcp	$\Delta_{(bcc\_fcc)}$	$\Delta_{(bcc\_hcp)}$	$\Delta_{(fcc\_hcp)}$	bcc	
Li	−3.298	−6.569	−6.570	−0.006	−0.553	−0.547	−211.135	−712.583
Na	−2.253	−4.532	−4.533	0.006	−0.371	−0.377	−652.706	−2202.883
K	−1.858	−3.762	−3.7805	0.011	−0.299	−0.310	−120,995	−408,359

For each of these elements, the hcp form remains the most stable, although transitions between structures are possible with temperature variation. Lithium remains the most stable, followed by sodium and potassium.

The transition order is given as follows: $\Delta_{(bcc\_fcc):Li<Na<K;}$ $\Delta_{(bcc\_hcp):Li<K<Na}$; $\Delta_{(fcc\_hcp):Li<Na<K}$ lithium has the lowest energy for each of its transitions compared to sodium and potassium.

The calculated transition energies show that lithium transits preferentially from the BCC structure to the hexagonal structure, increasing from 2 to 6 (gaining 4 atoms per transition) atoms per cell, while sodium transits favourably from the CFC structure to the hexagonal structure, increasing from 4 to 6 atoms. Finally, the transition of potassium from the BCC structure to the CFC structure is the most difficult to achieve.

b) Mesh parameters

The crystal parameters giving the size of each of these structures and their multiplicities were calculated. The results are shown in Table 5.

Potassium has a considerable volume compared to sodium and lithium, and this order of magnitude is maintained whatever the crystallographic structure.

These results were in line with the theory, so we proceeded to simulate the battery on the anode.

4.2. Physical Properties

Choice of operating temperatures

Our study requires the tracking of particles around the melting temperature, on the understanding that at this temperature several phenomena become interesting, particularly the diffusion of particles in a system.

For this reason, we have arbitrarily chosen three (3) consecutive temperatures to monitor the behaviour of the physical quantities. These temperatures are shown in the Table 6 below:

Allures of physical quantities

All the physical quantities studied (of all the elements), see Figure 2, have the same appearance whatever the order of multiplicity 4*4*4 and 6*6*6, so we present here that of lithium to explain the diffusion phenomenon observed.

a) Lithium curves

This Figure 2 shows us the behaviour of the temperature drop between 450 K and about 200 K, at which temperature the kinetic energy becomes lower and

Table 5. Crystalline parameters.

elements						triclinic					
	1*1*1					4*4*4			6*6*6		
	bcc	fcc		hcp		bcc					
Li	3.487	4.408	3.117	5.399	5.090	13.951	13.951	13.951	20.927	20.927	20.927
Na	4.329	5.549	3.923	6.796	6.407	15.809	13.691	113.707	23.713	20.536	170.561
K	5.427	6.89	5.034	8,719	8,220	20,150	17,451	32,128	30,226	26,176	48,193

Table 6. Choice of study temperatures.

elements	**Li**	**Na**	**K**
Melting point (˚C)	**180.54**	**97.720**	**63.380**
T (K)	**450**	**350**	**330**
	400	**330**	**315**
	350	**300**	**300**

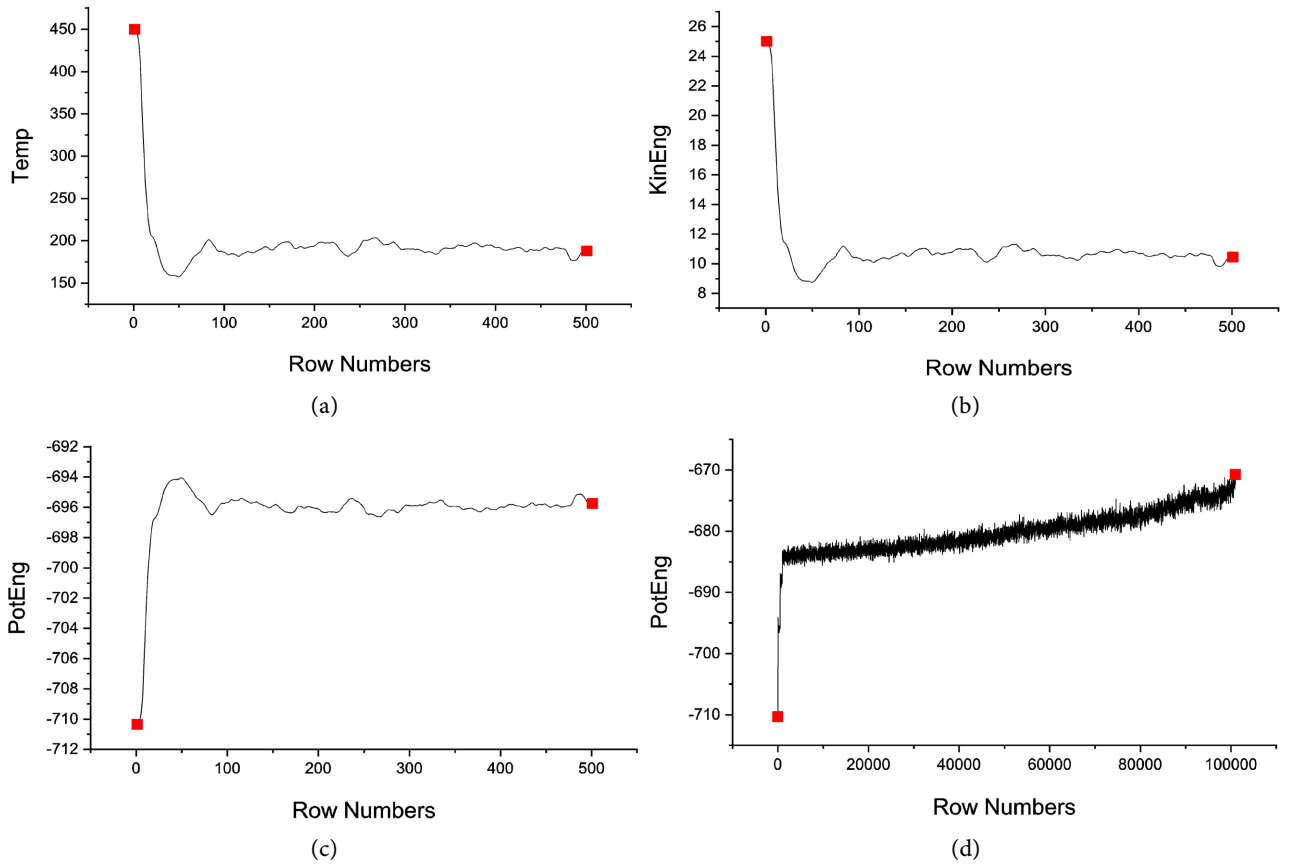

Figure 2. (a) Temperature; (b) Kinetic energy; (c) Potential energy.

lower, reflecting the low activity of the particles between (200 − 100,000) × 0.001 s = 99.8 s. This immobility is reflected by the increase in the interaction potential between the particles, which is retained more and more around 200 K.

This suggests that the closer we are to the melting temperature, the greater the extent of diffusion.

These results, in Table 7, show us how many times lithium remains the order of multiplicity for diffusion, since the greatest kinetic energy is reached at the highest temperature close to fusion.

b) Potassium

For potassium, we studied the behaviour of physical quantities for multiplicities without and with a gap. The results are presented in Table 8.

We can say that the 4 × 4 × 4 structures with a gap and without a gap are almost similar, although some differences are observed in favour of one over the other:

- (Ec, Pre): reaches 5.417 with a pressure of 8014.3164 at a temperature of 330 K compared with (5.374, 7499.723) around 315 K for 4 × 4 × 4;
- (Ec, Pre): (18.384, 7844.761) around 315 as much as (18.342, 7849.907) for the 6x6x6 multiplicity.

c) Sodium

The table below shows the physical quantities for sodium for multiplicities with a gap.

(Ec, Pre) is reached (24.484, 14500.312) around 330 K for 4 × 4 × 4 and (87.858, 14873.777) around350 K for 6 × 6 × 6. This information, in Table 9, tells us that around the melting point the scattering behaviour becomes increasingly important as the multiplicity increases.

4.3. Chemical Properties

a) the case of potassium

The behaviour shown in this Figure 3, from Table 10, shows us how often structures with a gap follow an order of magnitude, whereas structures without a gap are as if random over a considerable temperature range (15 K for potassium). However, the value of the diffusion coefficient is considerable in structures with a gap.

As a result of these observations, we reduced our work to structures with gaps for the other study elements, sodium and lithium.

b) case of sodium

This Figure 4, from Table 11, clearly shows the dual behaviour of diffusion at low multiplicity, which tends to disappear as the multiplicity increases. However, for sodium, diffusion is greater for 4 × 4 × 4 than for 6 × 6 × 6.

c) the case of lithium

This Figure 5, from Table 12, for lithium suggests that around non-consecutive temperatures, the behaviour of diffusion remains disturbed.

On the whole, it is preferable to carry out this study for close temperatures.

4.4. Analysis

Our overall analysis leads us to the 6*6*6 multiplicity structures, which show the most interesting results of all the structures.

Table 7. Temperature, pressure, kinetic energies, potential energies, total energies Lithium with and without gap.

			Time	Temp	Press	Ec	Epot	Etot
Li with a vacancy $(Li\ ion)^+$	444	300	0.0	300	5439.137	4.886	−209.125	−204.239
			0.5	134.152	−11026.102	2.184	−206.415	−204.230
			1.0	300	−3350.484	4.886	−204.633	−199.747
			101.0	265.101	−432.993	4.317	−203.161	−198.844
		400	0.0	400	6099.608	6.5147	−209.125	−202.610
			0.5	155.793	−6308.785	2.537	−205.143	−202.605
			1.0	400	−2579.023	6.514	−203.059	−196.544
			101.0	451.680	−4762.139	7.356	−200.096	−192.739
		450	0.0	450	6429.844	7.329	−209.125	−201.796
			0.5	179.970	−5463.863	2.931	−204.735	−201.804
			1.0	450	−2243.680	7.329	−202.583	−195.254
			101.0	466.714	622.322	7.601	−196.219	−188.618
	666	300	0.0	300	5790.878	16.674	−710.340	−693.665
			0.5	134.068	−8101.725	7.451	−701.104	−693.653
			1.0	300	−4218.324	16.674	−694.958	−678.284
			101.0	275.306	3995.076	15.302	−691.534	−676.232
		400	0.0	400	6458.727	22.232	−710.340	−688.107
			0.5	168.071	−4233.916	9.341	−697.440	−688.098
			1.0	400	−1851.984	22.232	−689.616	−667.383
			101.0	474.134	852.183	26.353	−677.133	−650.780
		450	0.0	450	6792.652	25.011	−710.340	−685.328
			0.5	187.892	−4004.124	10.443	−695.747	−685.303
			1.0	450	229.844	25.011	−688.200	−663.188
			101.0	497.919	−2611.638	27.675	−670.744	−643.069

Table 8. Temperature, pressure, kinetic energies, potential energies, total energies Potassium with and without gap.

			Time	Temp	Press	Ec	Epot	Etot
K without vacancy	444	300	0.0	300	7409.448	4.924	−117.683	−112.758
			0.5	154.369	7514.11	2.534	−115.292	−112.758
			1.0	300	7809.690	4.924	−113.822	−108.897
			101.0	240.171	7282.378	3.942	−112.857	−108.914
		315	0.0	315	7437.075	5.171	−117.683	−112.512
			0.5	163.929	7743.651	2.691	−115.203	−112.512
			1.0	315	7867.574	5.171	−113.883	−108.712
			101.0	294.871	7835.018	4.840	−113.520	−108.680

Continued

K without vacancy	666	330	0.0	330	7464.703	5.417	−117.683	−112.266
			0.5	174.341	7555.200	2.861	−115.128	−112.266
			1.0	330	8014.316	5.417	−113.476	−108.059
			101.0	324.682	7586.541	5.330	−113.380	−108.050
		300	0.0	300	7412.51	16.713	−397.182	−380.468
			0.5	168.125	7697.949	9.366	−389.835	−380.468
			1.0	300	7923.687	16.713	−385.186	−368.473
			101.0	250.132	7661.543	13.935	−382.349	−368.414
		315	0.0	315	7440.290	17.549	−397.182	−379.633
			0.5	177.105	7604.099	9.866	−389.500	−379.633
			1.0	315	7859.485	17.549	−389.500	−371.951
			101.0	264.137	7772.966	14.715	−381.554	−366.839
		330	0.0	330	7468.071	18.384	−397.182	−378.797
			0.5	184.053	7687.743	10.253	−389.049	−378.796
			1.0	330	7844.761	18.384	−384.085	−365.700
			101.0	281.773	7525.943	15.697	−381.320	−365.622
K with a vacancy $(K\ ion)^+$	444	300	0.0	300	7186.102	4.886	−116.547	−111.661
			0.5	158.395	7265.987	2.579	−114.240	−111.660
			1.0	300	7065.459	4.886	−112.776	−107.890
			101.0	272.360	7219.258	4.435	−112.299	−107.863
		315	0.0	315	7213.512	5.130	−116.547	−111.417
			0.5	166.916	7223.840	2.718	−114.135	−111.416
			1.0	315	6964.100	5.130	−112.726	−107.596
			101.0	292.595	7499.723	4.765	−112.344	−107.579
		330	0.0	330	7240.922	5.374	−116.547	−111.172
			0.5	177.721	7432.616	2.894	−114.067	−111.172
			1.0	330	7466.962	5.374	−112.719	−107.345
			101.0	305.347	7202.581	4.973	−112.318	−107.345
	666	300	0.0	300	7346.333	16.674	−396.046	−379.371
			0.5	166.732	7624.267	9.267	−388.639	−379.371
			1.0	300	7797.776	16.674	−384.123	−367.449
			101.0	258.579	7853.161	14.372	−381.774	−367.402
		315	0.0	315	7374.049	17.508	−396.046	−378.537
			0.5	177.271	7500.419	9.853	−388.390	−378.537
			1.0	315	7910.886	17.508	−383.545	−366.037
			101.0	267.044	7849.907	14.842	−380.812	−365.970
		330	0.0	330	7401.765	18.342	−396.046	−377.704
			0.5	184.942	7582.012	10.279	−387.982	−377.702
			1.0	330	7715.945	18.342	−382.742	−364.400
			101.0	272.413	7800.747	15.141	−379.479	−364.338

Table 9. Temperature, pressure, kinetic energies, potential energies, total energies Sodium with and without gap.

			Time	Temp	Press	Ec	Epot	Etot
Na with a vacancy $(Na\ ion)^+$	444	300	0.0	300	13478.262	22.258	−639.343	−617.085
			0.5	137.250	13967.083	10.183	−627.267	−617.084
			1.0	300	14120.624	22.258	−622.053	−599.795
			101.0	278.717	14331.399	20.679	−620.240	−599.560
		330	0.0	330	13590.763	24.484	−639.343	−614.859
			0.5	156.404	14068.836	11.604	−626.463	−614.858
			1.0	330	14500.312	24.484	−621.044	−596.560
			101.0	279.422	14167.543	20.731	−617.234	−596.502
		350	0.0	350	13665.764	25.968	−639.343	−613.375
			0.5	166.939	13952.122	12.386	−625.761	−613.375
			1.0	350	14217.480	25.968	−620.035	−594.066
			101.0	311.692	14110.471	23.126	−617.048	−593.922
	666	300	0.0	300	13546.751	75.306	−2161.031	−2085.724
			0.5	140.103	13983.88	35.169	−2120.888	−2085.718
			1.0	300	14513.573	75.306	−2106.582	−2031.275
			101.0	257.751	14265.607	64.701	−2095.618	−2030.916
		330	0.0	330	13659.528	82.837	−2161.031	−2078.193
			0.5	156.493	14135.713	39.283	−2117.472	−2078.189
			1.0	330	14600.615	82.837	−2101.777	−2018.940
			101.0	280.637	14136.809	70.446	−2089.296	−2018.849
		350	0.0	350	13734.713	87.858	−2161.031	−2073.173
			0.5	167.226	14155.913	41.977	−2115.146	−2073.169
			1.0	350	14873.777	87.858	−2098.420	−2010.562
			101.0	304.999	14625.596	76.562	−2086.578	−2010.016

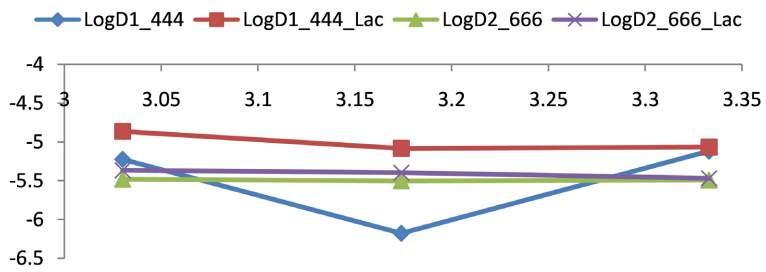

Figure 3. Diffusion coefficients with and without potassium gap.

Table 13 shows that it is preferable to use sodium as an anode because of its lower activation energy value, which results in greater chemical reduction than lithium and potassium.

Table 10. Diffusion coefficient and activation energy Potassium with and without gap.

(a)

444 without gaps				
T	**1000/T**	**D**	**logD**	**Eact**
300	3.333	7.577e−09	−5.120	4.11e−11
315	3.174	6.64e−09	−6.177	
330	3.030	5.969e−09	−5.224	−1.12e−21

(b)

444 with gap				
T	**1000/T**	**D**	**logD**	**Eact**
300	3.333	8.565e−09	−5.067	−9.26e−21
315	3.174	8.254e−09	−5.083	
330	3.030	1.362e−08	−4.865	3.03e−20

(c)

666 without gaps				
T	**1000/T**	**D**	**logD**	**Eact**
300	3.333	3.216e−09	−5.492	−1.886e−21
315	3.174	3.147e−09	−5.502	
330	3.030	3.303e−09	−5.481	4.63e−21

(d)

666 with gap				
T	**1000/T**	**D**	**logD**	**Eact**
300	3.333	3.397e−09	−5.468	1.436e−20
315	3.174	4.007e−09	−5.397	
330	3.030	4.302e−09	−5.366	6.80e−21

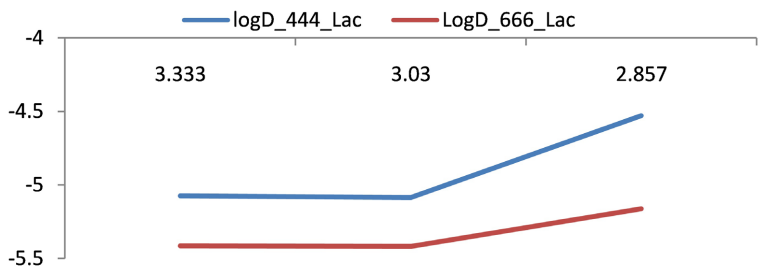

Figure 4. Diffusion coefficients with and without sodium gap.

5. Conclusions

In this work, we used the MEAM potential of the chemical elements Li, Na and K to calculate the diffusion coefficient and their activation energies; for the anions, we created a case gap by deleting an atom in the high-multiplicity structure.

Table 11. Diffusion coefficient and sodium activation energy with and without a gap.

(a)

444 with gap				
T	**1000/T**	**D**	**logD**	**Eact**
300	3.333	8.423e−09	−5.074	−1.18E-21
330	3.030	8.208e−09	−5.085	
350	2.857	2.953e−08	−4.529	1.02E−19

(b)

666 with gap				
T	**1000/T**	**D**	**logD**	**Eact**
300	3.333	3.843e−09	−5.415	−3.33E−22
330	3.030	3.815e−09	−5.418	
350	2.857	6.881e−09	−5.162	4.70E−20

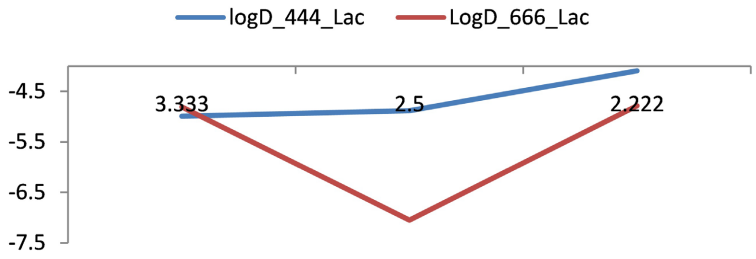

Figure 5. Diffusion coefficients with and without lithium gap.

Table 12. Diffusion coefficient and lithium activation energy with and without a gap.

(a)

666 without gaps				
T	**1000/T**	**D**	**logD**	**Eact**
300	3.333	1.556e−08	−4.807	−9.26E−21
400	2.5	8.9e−09	−7.050	
450	2.222	1.639e−08	−4.785	3.03E−20

(b)

444 without gaps				
T	**1000/T**	**D**	**logD**	**Eact**
300	3.333	1.016e−08	−4.993	4.11E−21
400	2.5	1.302e−08	−4.885	
40	2.222	8.143e−08	−4.089	9.11E−20

We give our choice on all our calculations as well as the basic data of our elements. We compare structures with odd multiplicity against those with even multiplicity. All the results are presented in the table below:

Table 13. Comparison of diffusion coefficients and activation energies.

Elements	structure	Melting temperature	Temperature operational	D	Ea
Na	**6*6*6**	**97.720**	**350**	**3.843e−09**	5.830e−22
			330	**3.815e−09**	
K		**63.380**	315	4.007e−09	6.796e−21
			330	4.302e−09	
Li		**180.54˚C**	**400**	**8.9e−09**	3.034e−20
			450	**1.639e−08**	

- For the anode, lithium reaches its best diffusion point at around 450 K, followed by potassium and finally sodium. It would be preferable to use potassium as the anode, because of its low melting point;
- Lithium has the highest activation energy, followed by potassium and sodium.

It would be preferable to use sodium as an anode in some cases.

Conflicts of Interest

The authors declare no conflicts of interest regarding the publication of this paper.

References

[1] John Wiley & Sons (2015) Energy Science & Engineering. The Society of Chemical Industry Ltd., London.

[2] El Idi, M.M., Karkri, M., Tankari, M.A., Larouci, C., Azib, T., *et al.* (2020) Caractérisation du comportement thermique des batteries Li-ion en vue d'une gestion optimale passive. Congrès Annuel de la Société Française de Thermique, Belfort, France.

[3] Ianniciello, L., Biwole, P.H. and Achard, P. (2017) Gestion thermique des batteries Li-ion par l'utilisation de matériaux à changement de phase et d'air en convection forcée. *Congrès français de thermique Thermique mer et océans*, Marseille, France.

[4] Bancelin, M. (2012) Mise au point et étude du comportement d'un séparateur innovant pour batterie lithium-ion à électrode négative à conversion. Thèse de doctorat en Sciences. Chimie des matériaux. Sciences des matériaux

[5] Duclos, L. (2016) Vers l'éco-conception des piles à combustible: Développement d'un procédé de recyclage des catalyseurs des systèmes de PEMFC à base de platinepar. Thèse de doctorat en Mécanique des fluides, procédés, énergétique, Soutenue à l'Université Grenoble Alpes (ComUE).

[6] Jiri, B., Pavel, R. and Mohamed, K. (2007) Recyclage des dechets d'extraction et de traitement des matieres minerales-exemple du recyclage des dechets d'exploitation des minerais d'etain et de tungstene. https://www.researchgate.net/publication/281095058_RECYCLAGE_DES_DECHETS_D'EXTRACTION_ET_DE_TRAITEMENT_DES_MATIERES_MINERALES_-EXEMPLE_DU_RECYCLAGE_DES_DECHETS_D'EXPLOITATION_DES_MINERAIS_D'ETAIN_ET_DE_TUNGSTENE

[7] Chipot, C. (2002) Les methodes numeriques de la dynamique moleculaire, Equipe de chimie et & biochimie theoriques, Unite Mixte de Recherche CNRS/UHP 7565. Institut Nanceien de Chimie Moleculaire, Universite Henri Poincare, Vandœuvre-l'es-Nancy, France.

[8] Jacques, T. (2004) L'algorithme de Newton-Hooke. https://www.researchgate.net/publication/328304992_L'algorithme_de_Newton-Hooke

[9] Owen, D.R.J., Wriggers, P. and Zohdi, T.I. (2019) Time Integration Errors and Energy Conservation Properties of the Stormer Verlet Method Applied to Mpm. https://upcommons.upc.edu/bitstream/handle/2117/186810/Particles_2019-50-Time%20integration%20errors.pdf

[10] Grønbech-Jensen, N. and Farago, O. (2013) A Simple and Effective Verlet-Type Algorithm for Simulating Langevin Dynamics. *Molecular Physics*, **111**, 983-991.

[11] Lee, B.-J., Baskes, M.I., Hanchul, K. and Yang, K.C. (2001) Second Nearest-Neighbor Modified Embedded Atom Method Potentials for BCC Transition Metal. *Physical Review B*, **64**, 184102. https://doi.org/10.1103/PhysRevB.64.184102

[12] Jelinek, B., Groh, S., Horstemeyer, M.F., Houze, J., Kim, S.G., Wagner, G.J., Moitra, A. and Baskes, M.I. (2012) MEAM Potentials for Al, Si, Mg, Cu, and Fe Alloys. *Physical Review B*, **85**, 245102. https://doi.org/10.1103/PhysRevB.85.245102

[13] Laforgue-Kantzer, D., Laforgue, A. and Khanh, T.C. (1972) Sens physique de l'énergie d'activation de conductibilité. *Electrochimica Acta*, **17**, 151-159. https://doi.org/10.1016/0013-4686(72)85016-3

[14] Aghfir, A., Akkad, S., Rhazi, M., Kane, C.S.E. and Kouhila, M. (2008) Détermination du coefficient de diffusion et de l'énergie d'activation de la menthe lors d'un séchage conductif en régime continu. *Revue des Energies Renouvelables*, **11**, 385-394.

[15] Goldberg, I.B. and Weger, M. (1972) The Electronic Band Structure of v_3ga and v_3si. *Journal de Physique Colloques*, **33**, C3-223-C3-233. https://doi.org/10.1051/jphyscol:1972333

[16] Conan, A. and Goureaux, G. (1973) Calcul de la largeur de bande et de l'énergie d'échange du quasi-electron dans les métaux simples. *Physica*, **70**, 165-174. https://doi.org/10.1016/0031-8914(73)90286-3